

Selective Molecular Assembly Patterning: A New Approach to Micro- and Nanochemical Patterning of Surfaces for Biological Applications

Roger Michel,[†] Jost W. Lussi,[‡] Gabor Csucs,[§] Ilya Reviakine,[†] Gaudenz Danuser,[§] Brigitte Ketterer,^{||} Jeffrey A. Hubbell,[‡] Marcus Textor,^{*,†} and Nicholas D. Spencer[†]

Laboratory for Surface Science and Technology, Institute for Biomedical Engineering, and BioMicroMetricsGroup (BMMG), ETH Zurich, Wagistrasse 2, CH-8952 Schlieren, Switzerland, and Paul-Scherrer Institute, PSI Villigen, CH-5232 Villigen PSI, Switzerland

Received November 26, 2001. In Final Form: January 28, 2002

A novel patterning technique based on selective self-assembly of alkane phosphates on metal oxide surfaces is presented. Standard photolithography was used to create patterns of titanium dioxide within a matrix of silicon dioxide. Alkane phosphates were found to self-assemble on TiO₂, but not on SiO₂, surfaces. Subsequent adsorption of poly(L-lysine)-*g*-poly(ethylene glycol) (PLL-*g*-PEG) rendered the exposed SiO₂ surface resistant to protein adsorption. X-ray photoelectron spectroscopy and time-of-flight secondary ion mass spectrometry were employed to monitor the assembly processes. Protein-adsorption studies by means of fluorescence microscopy conclusively established that the resulting surfaces displayed protein-adhesive, alkyl phosphate modified TiO₂ features, arranged within a protein-resistant PLL-*g*-PEG-modified SiO₂ matrix. Human foreskin fibroblasts, incubated in a serum-containing medium, were found to selectively attach to the protein-adhesive areas, where they developed focal contacts. No interaction of cells with the PLL-*g*-PEG-coated SiO₂ areas was evident for at least 14 days. This patterning approach, termed selective molecular assembly patterning, is considered to be suitable for reproducible and cost-effective fabrication of biologically relevant chemical patterns over large areas.

1. Introduction

A variety of patterning techniques is currently available for studying the effects of chemical patterning and topographical microstructuring of surfaces on cell attachment, growth, differentiation, and death.^{1–3} Interest in these effects is driven in part by the need to investigate, control, and improve implant–body interactions and implant integration. Moreover, the growing demand in biosensor technology for high-density, high-sensitivity, multianalyte chips can only be met with precise and reproducible patterning methodologies that allow a controlled juxtaposing of chemically distinct, active areas. The similarity of needs and constraints between the implant and the biosensor fields has led to the development of chemical,^{2,4,5} topochemical,⁶ and topographical^{7,8} patterning methodologies that are applicable to both areas.

Surfaces can be chemically patterned using a number of techniques, such as microcontact printing,^{2,9} microfluidic patterning,¹⁰ photolithography,¹¹ and photodegradation^{12,13} or photoactivation¹⁴ of self-assembled monolayers (SAMs) that have been shown to present termini which resist protein adsorption¹⁵ and cell attachment.¹⁶ Although these patterning techniques have proven to be well suited for specific, mostly benchtop applications, they suffer from a number of limitations. While the nonphotolithographic techniques meet the criteria outlined above for spatial control, they are often incompatible with standard industrial processes, since the elastomeric stamps^{2,10,17} are difficult to use reproducibly over large areas, transfer contaminants,¹⁸ and degrade over time. Current photolithographic techniques that circumvent the use of polymeric stamps require complex chemistry,^{11,14} while sol-

* Corresponding author: Dr. Marcus Textor, ETH Zürich, Laboratory for Surface Science and Technology, Wagistrasse 2, CH-8952 Schlieren, Switzerland. Phone: +41 (0)1 632 64 51. Fax: +41 (0)1 633 10 48. E-mail: textor@surface.mat.ethz.ch.

[†] Laboratory for Surface Science and Technology, ETH Zurich.

[‡] Institute for Biomedical Engineering, ETH Zurich.

[§] BioMicroMetricsGroup (BMMG), ETH Zurich.

^{||} Paul-Scherrer Institute, PSI Villigen.

(1) Blawas, A. S.; Reichert, W. M. *Biomaterials* **1998**, *19*, 595–609.

(2) Chen, C. S.; Mrksich, M.; Huang, S.; Whitesides, G. M.; Ingber, D. E. *Science* **1997**, *276*, 1425–1428.

(3) Ito, Y. *Biomaterials* **1999**, *20*, 2333–2342.

(4) Blawas, A. S.; Oliver, T. F.; Pirrung, M. C.; Reichert, W. M. *Langmuir* **1998**, *14*, 4243–4250.

(5) Whitesides, G. M.; Ostuni, E.; Takayama, S.; Jiang, X. Y.; Ingber, D. E. *Annu. Rev. Biom. Eng.* **2001**, *3*, 335–373.

(6) Shi, H. Q.; Tsai, W. B.; Garrison, M. D.; Ferrari, S.; Ratner, B. D. *Nature* **1999**, *398*, 593–597.

(7) Inoue, A.; Ishida, T.; Choi, N.; Mizutani, W.; Tokumoto, H. *Appl. Phys. Lett.* **1998**, *73*, 1976–1978.

(8) Brunette, D. M. *The effect of surface topography on cell migration and adhesion*; Ratner, B. D., Ed.; Elsevier Science Publishers B. V.: Amsterdam, 1988; pp 203–217.

(9) Bernard, A.; Delamarche, E.; Schmid, H.; Michel, B.; Bosshard, H. R.; Biebuyck, H. *Langmuir* **1998**, *14*, 2225–2229.

(10) Delamarche, E.; Bernard, A.; Schmid, H.; Michel, B.; Biebuyck, H. *Science* **1997**, *276*, 779–781.

(11) McFarland, C. D.; Thomas, C. H.; DeFilippis, C.; Steele, J. G.; Healy, K. E. *J. Biomed. Mater. Res.* **2000**, *49*, 200–210.

(12) Yang, X. M.; Peters, R. D.; Kim, T. K.; Nealey, P. F.; Brandow, S. L.; Chen, M. S.; Shirey, L. M.; Dressick, W. J. *Langmuir* **2001**, *17*, 228–233.

(13) Corey, J. M.; Wheeler, B. C.; Brewer, G. J. *IEEE Trans. Biomed. Eng.* **1996**, *43*, 944–955.

(14) Yang, Z. P.; Frey, W.; Oliver, T.; Chilkoti, A. *Langmuir* **2000**, *16*, 1751–1758.

(15) Ostuni, E.; Chapman, R. G.; Liang, M. N.; Meluleni, G.; Pier, G.; Ingber, D. E.; Whitesides, G. M. *Langmuir* **2001**, *17*, 6336–6343.

(16) Chapman, R. G.; Ostuni, E.; Liang, M. N.; Meluleni, G.; Kim, E.; Yan, L.; Pier, G.; Warren, H. S.; Whitesides, G. M. *Langmuir* **2001**, *17*, 1225–1233.

(17) Patel, N.; Bhandari, R.; Shakesheff, K. M.; Cannizzaro, S. M.; Davies, M. C.; Langer, R.; Roberts, C. J.; Tendler, S. J. B.; Williams, P. M. *J. Biomater. Sci., Polym. Ed.* **2000**, *11*, 319–331.

(18) Yang, Z. P.; Belu, A. M.; Liebmann-Vinson, A.; Sugg, H.; Chilkoti, A. *Langmuir* **2000**, *16*, 7482–7492.

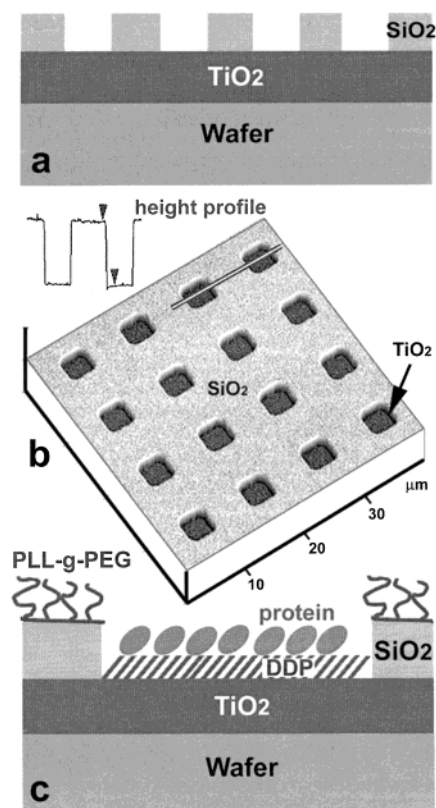


Figure 1. A schematic illustration of the SMAP methodology. (a) Sample exhibiting a material contrast, produced using common photolithographic techniques. TiO_2 squares within the SiO_2 matrix are shown. (b) An atomic force microscope image of the surface shown in (a). TiO_2 squares are located ~ 35 nm below the SiO_2 matrix (inset: a height profile of the surface). (c) Schematic view of the surface after the surface modification procedures: DDP on TiO_2 , protein on DDP, and PLL-*g*-PEG on SiO_2 , with the poly(lysine) backbone lying flat on the surface and PEG chains extending away from it.

vents used in conventional photolithography may denature or degrade deposited bio-organic layers.¹

The preceding discussion indicates the demand for a technology that allows chemical patterning into areas that are distinctly protein and cell adhesive or nonadhesive. This technology should also be free of the limitations imposed by the use of polymeric stamps or photolithographic processes on organic overlayers. Selective molecular assembly patterning (SMAP) introduced in this work meets these criteria.

SMAP is based on a combination of lithographic structuring of metal oxide surfaces (Figure 1a,b) with the selective self-assembly of organic molecules, namely, alkyl phosphates^{19,20} and poly(L-lysine)-*g*-poly(ethylene glycol) (PLL-*g*-PEG),²¹ on distinct metal oxide surfaces. Alkyl phosphates are known to self-assemble on metal oxide substrates, such as TiO_2 , from aqueous solutions,²² rendering them hydrophobic. PLL-*g*-PEG, however, renders negatively charged metal oxide surfaces, such as SiO_2 , resistant to protein adsorption and cell attachment.^{21,23,24}

(19) Bram, C.; Jung, C.; Stratmann, M. *Fresenius' J. Anal. Chem.* **1997**, *358*, 108–111.

(20) Textor, M.; Ruiz, L.; Hofer, R.; Rossi, A.; Feldman, K.; Hahner, G.; Spencer, N. D. *Langmuir* **2000**, *16*, 3257–3271.

(21) Elbert, D. L.; Hubbell, J. A. *Chem. Biol.* **1998**, *5*, 177–183.

(22) Hofer, R.; Textor, M.; Spencer, N. D. *Langmuir* **2001**, *17*, 4014–4020.

(23) Kenausis, G. L.; Voros, J.; Elbert, D. L.; Huang, N. P.; Hofer, R.; Ruiz-Taylor, L.; Textor, M.; Hubbell, J. A.; Spencer, N. D. *J. Phys. Chem. B* **2000**, *104*, 3298–3309.

Thus, by sequentially adsorbing alkyl phosphate and PLL-*g*-PEG onto a suitably structured surface consisting of a pattern of different adsorbing oxide regions (such as a TiO_2 pattern surrounded by a matrix of SiO_2), a surface exhibiting a pattern of protein-adhesive regions (alkyl phosphate) surrounded by a protein-resistant matrix (PLL-*g*-PEG) can be prepared (Figure 1c).

The spatial resolution of SMAP is limited by the lithographic approach used in the patterning of metal oxide substrates, which can easily reach nanometer length scales.²⁵ Recently introduced processes suitable for patterning metal oxide surfaces in the nanometer range, such as colloidal lithography,²⁶ hot embossing,²⁷ or template synthesis,²⁸ can also be applied in combination with SMAP, to generate large-scale, affordable, biologically relevant chemical patterns.

2. Materials and Methods

2.1. Substrate Preparation. Two kinds of substrates were employed for the investigation of the selective adsorption on SiO_2 and TiO_2 surfaces. Silicon wafer pieces (1 cm²) or glass cover slips (Plano GmbH, Germany), coated half with SiO_2 and half with TiO_2 , were used to quantitatively investigate the self-assembly processes. Additionally, whole 4 in. silicon (110) wafers were used to produce square patterns of $5 \times 5 \mu\text{m}^2$ and $60 \times 60 \mu\text{m}^2$, that were subsequently analyzed by imaging time-of-flight secondary ion mass spectrometry (ToF-SIMS) and used for protein-adhesion and cell-attachment experiments.

2.2. Substrate Coating. Four inch silicon (110) wafers (Wafernet GmbH, Germany) were sputter-coated with a 100 nm TiO_2 layer, followed by a 20 nm SiO_2 layer. The coated wafers were then used in subsequent photolithographic patterning steps (section 2.3). The 1 cm² silicon wafer pieces or glass coverslips were coated with a 12 nm SiO_2 layer, covered with aluminum foil to expose half of the slide, and coated with 12 nm of TiO_2 , to be used in surface modification steps (section 2.4). All coating steps were carried out with a Leybold dc-magnetron Z60 sputtering plant. The deposition and characterization of these oxide coatings have been described previously.²⁹

2.3. Patterning: Creating Material Contrast. A 30 nm aluminum hard mask was evaporated onto the TiO_2 - and SiO_2 -coated substrate surfaces with a Balzer BAK 600 coater.

A Shipley S1813 photoresist was spin-coated onto the aluminum layer with an STD5 Karl Süss spin coater at 4000 rpm for 25 s and baked at 90 °C for 60 s, resulting in a resist thickness of 1.3–1.5 μm . The resist was exposed to UV light through a suitable mask for 4–5 s using a MA6 Karl Süss mask aligner and developed with Shipley MF-84MX developer solution for 30 min.

After the photolithographic step, the resist pattern was transferred into the aluminum layer by wet etching³⁰ for 5 min. The resist was then stripped in a removal bath. After an additional cleaning step in acetone, the structured aluminum layer was used as a hard mask during the reactive ion etching (RIE) of silicon dioxide. The latter was carried out with an Oxford Plasma Lab 100, using a mixture of O_2 and CHF_3 , in a ratio of 3:40 sccm, at 100 mTorr, 300 K, and 100 W, for 180 s. The temperature was controlled at 300 ± 5 K with a liquid-nitrogen-cooled cryotable. The depth of the etching was measured with a Tencor Alpha-step profilometer. After the RIE, the aluminum hard mask was

(24) Huang, N. P.; Michel, R.; Voros, J.; Textor, M.; Hofer, R.; Rossi, A.; Elbert, D. L.; Hubbell, J. A.; Spencer, N. D. *Langmuir* **2001**, *17*, 489–498.

(25) Xia, Y. N.; Rogers, J. A.; Paul, K. E.; Whitesides, G. M. *Chem. Rev.* **1999**, *99*, 1823–1848.

(26) Hanarp, P.; Sutherland, D.; Gold, J.; Kasemo, B. *Nanostruct. Mater.* **1999**, *12*, 429–432.

(27) Schiff, H.; Heyderman, L. J.; Maur, M. A. D.; Gobrecht, J. *Nanotechnology* **2001**, *12*, 173–177.

(28) Schlöttig, F.; Textor, M.; Spencer, N. D.; Sekinger, K.; Schnaut, U.; Paulet, J. F. *Fresenius' J. Anal. Chem.* **1998**, *361*, 684–686.

(29) Kurrat, R.; Textor, M.; Ramsden, J. J.; Boni, P.; Spencer, N. D. *Rev. Sci. Instrum.* **1997**, *68*, 2172–2176.

(30) Büttenbach, S. *Mikromechanik: Einführung in Technologie und Anwendung*; Teubner: Stuttgart, 1991.

removed by wet etching,³⁰ and wafers were cleaned and dried thoroughly, protected with 1.3 μm of Shipley S1813 photoresist, transferred to an adhesive backing, and sawn into $10 \times 10 \text{ mm}^2$ pieces on a wafer-sawing machine (ESEC, Zug, Switzerland). Sawn samples were ultrasonically cleaned in hexane, ethanol, and water for 3 min each and stored until use. Immediately before the self-assembly processes, the samples were cleaned in an oxygen-plasma cleaner (Harrick Scientific Corp., Ossining, NY) for 2 min.

2.4. SMAP Patterning: Conversion of Material Contrast into Protein-Adhesion Contrast. It will be shown in the results section that the adsorption of the organic molecules described below is selective and creates a protein-adhesion contrast.

2.4.1. Selective Self-Assembly of Dodecyl Phosphate (DDP) on Titanium Oxide. Ammonium dodecyl phosphate, $\text{DDPO}_4(\text{NH}_4)_2$, was prepared as described previously.²² It was dissolved at a concentration of 0.5 mM in high-purity water at 50 °C, cooled to room temperature, and stored (for a maximum of 14 days) until used. Samples (1 cm^2) exhibiting material contrast, prepared as described in section 2.1, were immersed in 1 mL of $\text{DDPO}_4(\text{NH}_4)_2$ solution and incubated for 24 h, after which they were removed, rinsed with high-purity water, and blown dry in a stream of nitrogen.

2.4.2. Assembly of PLL-*g*-PEG. The PLL(20 kD)-*g*[3.5]-PEG-(2 kD) graft copolymer (based on PLL of MW 20 000 and PEG of MW 2000, with a grafting ratio of PLL/PEG of 3.5) was synthesized and characterized as previously described.²³ Patterned, DDP-coated samples, prepared as described above, were immersed in 1 mg/mL copolymer solution in Hepes Z1 buffer (10 mM 4-(2-hydroxyethyl)piperazine-1-ethanesulfonic acid, adjusted to pH 7.4 with 6 M NaOH, Fluka) for 15 min, washed with Hepes Z1 buffer and then with water, and dried with a stream of nitrogen. This step was performed in 24-well tissue-culture polystyrene plates for samples that were to be used in cell studies (section 2.5.2).

2.5. Protein Adsorption and Cell Attachment on Patterned Substrates. 2.5.1. Protein-Adsorption Experiments. The samples prepared as described in sections 2.4.1 and 2.4.2 were incubated in 40 $\mu\text{g}/\text{mL}$ Oregon Green labeled streptavidin (Molecular Probes, Eugene, OR) for 1 h and rinsed with Hepes Z1 buffer, washed with water, and blown dry. For X-ray photoelectron spectroscopy (XPS) and ToF-SIMS experiments, SMAP samples were subjected to full serum (Human Control Serum N, Hoffmann-La Roche, Switzerland) for 40 min instead of the fluorescently labeled streptavidin.

2.5.2. Cell-Attachment Experiments. Cell attachment was measured inside 24-well tissue-culture test plates (TPP, Switzerland). Glass cover slips, coated half with TiO_2 and half with SiO_2 , as well as Si wafers with 5×5 or $60 \times 60 \mu\text{m}^2$ protein-adhesive (TiO_2/DDP) squares in a protein-resistant ($\text{SiO}_2/\text{PLL-g-PEG}$) matrix (adhesion contrast, see sections 1 and 2) were used as substrates. Human foreskin fibroblasts (HFFs), kept under standard culture conditions, were plated onto substrates in Dulbecco's modified Eagle's medium (DMEM) containing Glutamax I (GIBCO Life Technologies) and sodium pyruvate, supplemented with 10% fetal bovine serum and a 1% antibiotic/antimycotic solution (GIBCO), at a seeding density of 5000 cells per cm^2 . The medium was exchanged twice a week for the length of the experiment.

After 20 h of incubation, cells were fixed with 4% neutral-buffered formalin/0.01% glutaraldehyde solution in phosphate-buffered saline (PBS) for 2 h at 4 °C and permeabilized with 0.1% Triton X100 in PBS for 5 min. After washing and blocking (1 h in a mixture of 1.5% bovine serum albumin and 0.005% Tween20 (Aldrich) in PBS, referred to hereafter as the blocking buffer), cells were incubated with the primary monoclonal mouse anti-human vinculin clone hVIN-1 dissolved 1:400 in blocking buffer for 1 h, washed, and incubated with a solution containing a secondary FITC-labeled goat anti-mouse antibody, rhodamine-labeled phalloidin (which binds to f-actin), and Hoechst/DAPI nuclear stain.

Finally, the cells were washed with PBS and mounted on microscope slides with Vectashield (Vector Labs, Burlingame, CA) for observation in an optical microscope. All chemicals for immunostaining were obtained from Sigma (St. Louis, MO), unless specified otherwise.

2.6. Sample Characterization. 2.6.1. X-ray Photoelectron Spectroscopy. All XPS spectra were recorded on a SAGE 100 (SPECS, Berlin, Germany) using nonmonochromatic Mg K α radiation with an energy of 240 W (12 kV, 20 mA), an electron takeoff angle of 90°, and electron-detector pass energies of 50 eV for survey and 14 eV for detailed spectra. For the high-resolution, detailed spectra, a reference Ag(3d_{5/2}) full width at half-maximum (fwhm) corresponds to 1.0 eV. During analysis, the base pressure remained below 5×10^{-8} mbar. All peaks were referenced to the C(1s) (hydrocarbon C-C, C-H) contribution at 285.0 eV.³¹

2.6.2. Time-of-Flight Secondary Ion Mass Spectrometry. Secondary ion mass spectra were recorded on a PHI 7200 time-of-flight secondary ion mass spectrometer in the mass range 0–200 *m/z*. Imaging ToF-SIMS was carried out with an indium liquid-metal primary ion gun at a current of ~2 mA. For imaging purposes, the gun was operated at 25 keV, at a pulse width of 10 ns. The mass resolution $\Delta M/M$ of the peak C_2H_3^+ at *m/z* 27 in positive ion mode remained around 500. All surfaces were scanned with a ~500 nm ion beam across $300 \times 300 \mu\text{m}^2$. No charge compensation was necessary for acquisition.

2.6.3. Fluorescence Microscopy. Fluorescence microscopy investigations of the modified surfaces and cell-surface interactions were carried out using a Zeiss LSM 510 confocal laser-scanning microscope. Three different laser lines were used in our experiments: Oregon Green and FITC probes were excited at 488 nm, and rhodamine phalloidin at 543 nm; the 633 nm line was used to visualize the surface contrast in reflection mode during the cell experiments. Either a $20 \times$ (0.4NA) LD Achroplan or a $40 \times$ (0.6NA) LD Achroplan objective was used for protein-adhesion experiments. Characterization of cell morphology was performed with a $63 \times$ (1.25NA) Plan-Neofluar oil-immersion objective.

3. Results

Samples, one half coated with SiO_2 and the other half with TiO_2 , were used for quantitative surface analysis after each of the surface treatment steps (cleaning, self-assembly, and polymer and protein adsorption, section 2). These samples exhibit material contrast on a macroscopic scale and are discussed in section 3.1. Micropatterned surfaces were subjected to identical surface modification procedures and characterized qualitatively by imaging ToF-SIMS (section 3.2) and fluorescence microscopy (section 3.3) and were used in the cell experiments (section 3.4). In both types of samples, material contrast (on a macroscopic or microscopic scale, Figure 1a) is converted into contrast with respect to protein adhesion (Figure 1c) via a series of surface modification steps (self-assembly of DDP, adsorption of PLL-*g*-PEG; section 2).

3.1. Characterization of the Macroscopically Patterned Surfaces. 3.1.1. X-ray Photoelectron Spectroscopy. XPS is commonly used to analyze and quantify surface chemical composition.³² Cleaned, oxygen-plasma-treated surfaces exhibited low C(1s) intensities (Figure 2a,b) on both SiO_2 and TiO_2 , indicating only minor hydrocarbon contamination (<10 atomic %). After exposure of the surface to the DDP solution, the C(1s) intensity increased significantly on the TiO_2 surface to an amount typical of a DDP SAM.²² No such increase was observed on the SiO_2 (Figure 2). Consistent with this observation, no phosphorus signal was detected on SiO_2 following exposure to the DDP solution, and the Si intensity remained unchanged (Figure 2d). In contrast, PLL-*g*-PEG was found to adsorb on both TiO_2/DDP and SiO_2 surfaces, as is indicated by the increase in both C(1s) and N(1s) intensities and the corresponding decrease in the substrate (Ti(2p) and Si(2p), respectively) intensities (Figure 2). On

(31) Wagner, C. D.; Riggs, W. M.; Davis, L. E.; Moulder, J. F.; Muilenberg, G. E. *Handbook of X-ray Photoelectron Spectroscopy*; Perkin-Elmer: Eden Prairie, MN, 1979.

(32) Vickerman, J. C. *Surface analysis – The principal techniques*; John Wiley: New York, 1997.

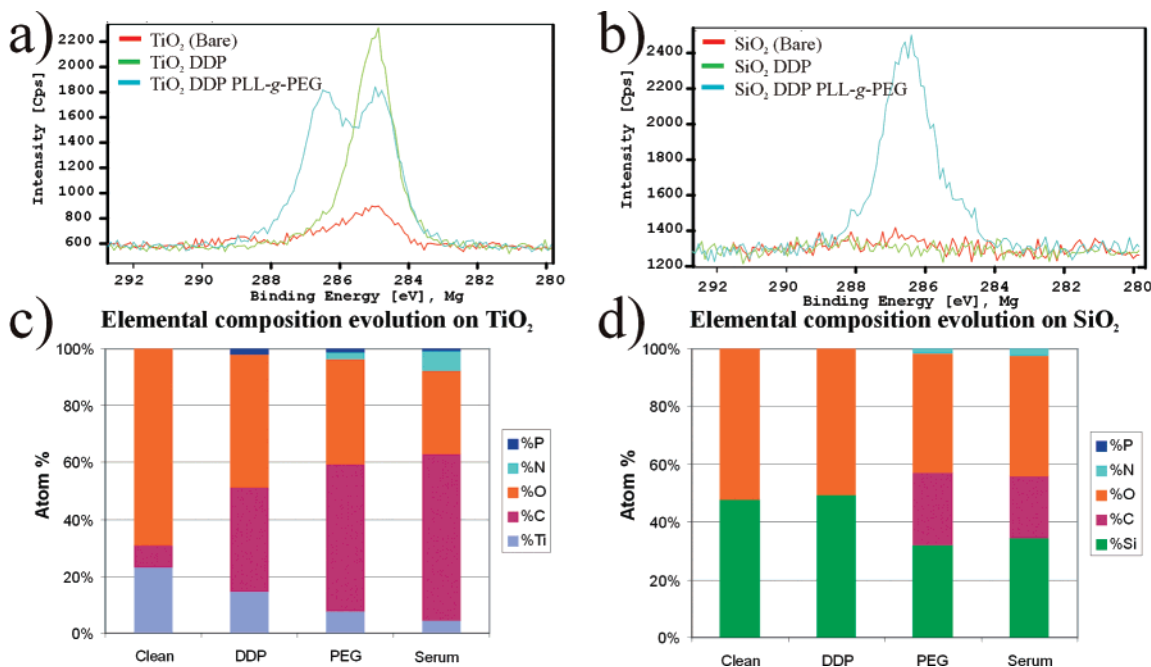


Figure 2. XPS spectra depicting the evolution of the C(1s) species on (a) TiO₂ and (b) SiO₂ areas of a sample. C(1s) is shown after cleaning and immersion in DDP and PLL-*g*-PEG. Elemental compositions of the surfaces are shown in (c) for TiO₂ and (d) for SiO₂, with serum immersion as an additional step.

SiO₂, deconvolution of the C(1s) peak revealed two components at 286.5 eV (C–O–C and C–O–H of PEG) and 285.0 eV (C–C and C–H of the lysine backbone), consistent with the chemical composition of the PLL-*g*-PEG molecule and an earlier detailed XPS study.²⁴ In the subsequent immersion step in full serum, protein replaced the PLL-*g*-PEG adsorbed onto the TiO₂/DDP (see below). The modified SiO₂/PLL-*g*-PEG surface remained unchanged (Figure 2d), while a decrease of the Ti(2p) as well as an increase in C(1s) and N(1s) (Figure 2c) signals indicated protein adsorption onto the TiO₂/DDP surface.

3.2. Characterization of the Patterned Surfaces

3.2.1. Time-of-Flight Secondary Ion Mass Spectrometry. ToF-SIMS³² is a valuable technique for qualitatively monitoring the adsorption of organic molecules onto surfaces, as it combines surface sensitivity with a high mass resolution. In addition, it can be used to investigate the localization of characteristic molecular ions with better than 1 μm lateral resolution, making it a valuable technique for monitoring surface modification steps on structured surfaces. When applied to the patterned substrates containing 60 × 60 μm² SiO₂ squares within a TiO₂ matrix, ToF-SIMS images (Figure 3) clearly indicated that Si⁺ ions (*m/z* 28, Figure 3b) were found exclusively within the 60 μm squares, while the Ti⁺ signal (*m/z* 47, Figure 3a) was only found in the surrounding matrix regions. The reverse was found on the samples with TiO₂ squares within a SiO₂ matrix (data not shown). To monitor the adsorption of DDP and PLL-*g*-PEG onto the substrate exhibiting material contrast, PO₄H₄⁺ (*m/z* 99) and C₃H₇O⁺ (*m/z* 59) ions were chosen. These ions are well separated from molecular ions originating from the metal oxide substrates and other organic fragments. A clear PO₄H₄⁺ signal (Figure 3c), indicating phosphate adsorption onto the TiO₂ areas, was detected on the substrates incubated with DDP for 24 h. Hydrocarbon fragments occurring in the same mass range as the PO₄H₄⁺ account for the slight increase in the intensity of the signal on the SiO₂ areas. On the other hand, PLL-*g*-PEG was found to adsorb onto both SiO₂ and TiO₂/DDP areas, as indicated by the presence of the C₃H₇O⁺ ion in both areas

(Figure 3d), consistent with the XPS findings (Figure 2a). Once exposed to serum, the amount of the C₃H₇O⁺ ion on the TiO₂/DDP surface was found to decrease (Figure 3e). On the other hand, peaks due to amino acid ions with the generic structure H₂N⁺=CH–R³³ appear on the TiO₂/DDP surface due to protein adsorption from the serum. These amino acid ions were not prominent on SiO₂. While the amount of the C₃H₇O⁺ ion decreased by 1 order of magnitude after protein adsorption, the amount of Ti⁺ ions detected remained constant. This suggests that the adsorbing proteins have replaced PLL-*g*-PEG on the DDP-functionalized regions.

3.3. Investigation of Protein Adsorption to Patterned Surfaces by Fluorescence Microscopy. Fluorescence microscopy was performed to obtain better insight into the adsorption behavior of proteins on the patterned TiO₂/SiO₂ oxide surfaces. Oregon Green labeled streptavidin was used as a model protein. Upon adsorption of the labeled streptavidin, the fluorescence signal ($3.8 \pm 0.09 \times 10^4$ au) was found to be localized on the hydrophobic, protein-adhesive DDP-coated TiO₂ 5 × 5 μm² squares (Figure 4), while the fluorescence intensity on the PLL-*g*-PEG-coated SiO₂ matrix ($6.4 \pm 0.5 \times 10^3$ au) remained close to the background level ($6.0 \pm 0.5 \times 10^3$ au, determined by photobleaching of selected areas).

This is illustrated with a fluorescence intensity profile across several features (Figure 4, inset). It is known from measurements with optical waveguide lightmode spectroscopy (OWLS)³⁴ that below 1 ng/cm² of protein is adsorbed on PLL-*g*-PEG,²⁴ while $\sim 50 \pm 3$ ng/cm² of streptavidin adsorbs on the DDP SAM (data not shown), resulting in a selectivity ratio (protein adsorbed on TiO₂/DDP over protein adsorbed on SiO₂/PLL-*g*-PEG) of at least ~ 50 . The fluorescence intensity values quoted above yield a contrast ratio of ~ 100 . The difference is likely to be caused by the lower sensitivity of OWLS.

Thus, the results of ToF-SIMS, XPS, and fluorescence measurements indicate that the material contrast present

(33) Mantus, D. S.; Ratner, B. D.; Carlson, B. A.; Moulder, J. F. *Anal. Chem.* **1993**, *65*, 1431–1438.

(34) Lukosz, W. *Sens. Actuators, B* **1995**, *29*, 37–50.

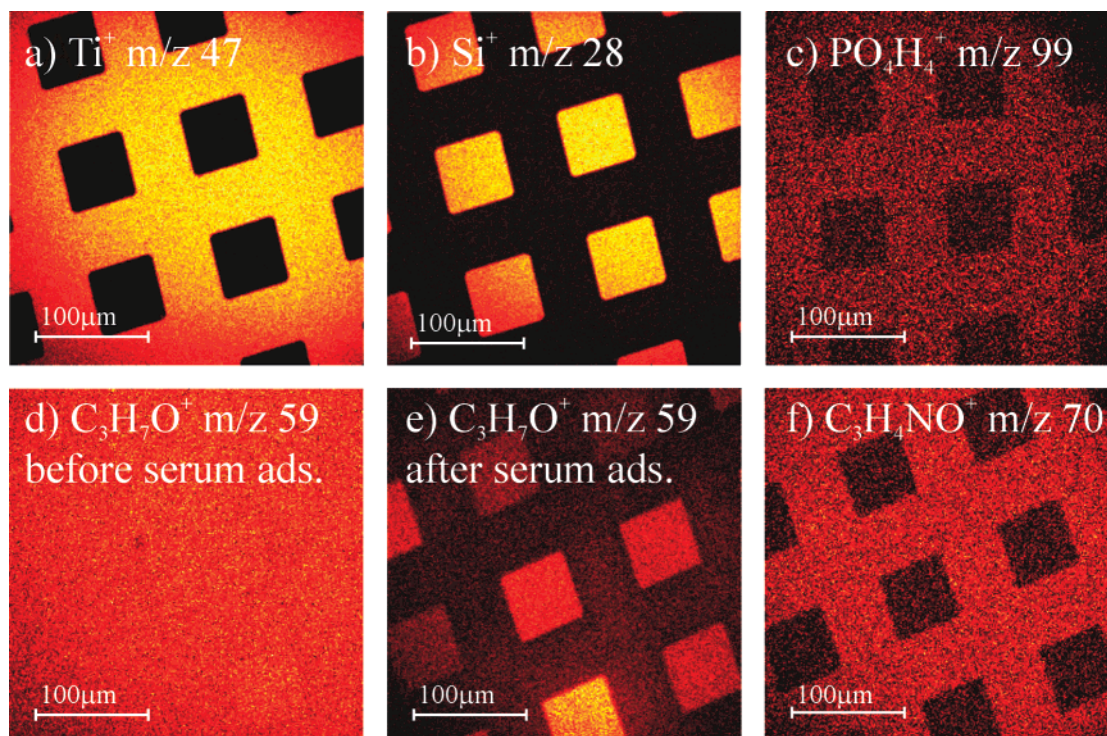


Figure 3. Positive ToF-SIMS images ($300 \times 300 \mu\text{m}^2$) of $60 \times 60 \mu\text{m}^2$ SiO_2 areas, $60 \mu\text{m}$ apart, in a matrix of TiO_2 . Positive ion maps are shown of (a) Ti^+ (m/z 47), (b) Si^+ (m/z 28), (c) PO_4H_4^+ (m/z 99), (d) $\text{C}_3\text{H}_7\text{O}^+$ (m/z 59) before serum adsorption, (e) $\text{C}_3\text{H}_7\text{O}^+$ (m/z 59) after serum adsorption, and (f) $\text{C}_3\text{H}_4\text{NO}^+$ (m/z 70), proline amino acid peak. The selectivity of the DDP on the TiO_2 is shown as well as the PLL-*g*-PEG adsorption to the whole surface and its subsequent removal by protein on the TiO_2 /DDP hydrophobic areas. A characteristic amino acid molecular ion, $\text{C}_3\text{H}_4\text{NO}^+$, was selected to show protein adsorption only to the TiO_2 /DDP.

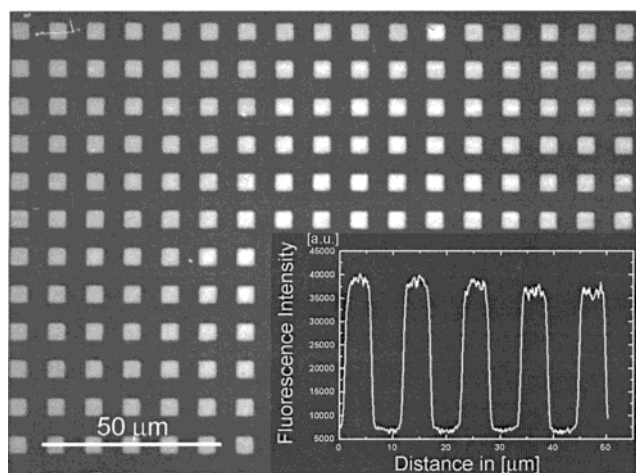


Figure 4. Fluorescence microscopy image on Oregon Green labeled streptavidin subjected to the SMAP-treated, $5 \times 5 \mu\text{m}^2$ TiO_2 in SiO_2 substrate. Streptavidin adsorption can only be observed on the TiO_2 /DDP spots, while the SiO_2 /PLL-*g*-PEG remains protein resistant. The inset shows the local distribution of fluorescence of the Oregon Green labeled streptavidin across the surface (in arbitrary units). A contrast of 100:1 was observed.

on the surface after the lithographic patterning steps (Figure 1a,b) was successfully converted to contrast with respect to protein adsorption (Figure 1c).

3.4. Cell Studies. In cell-culture assays, HFFs were incubated on three different adhesive/nonadhesive pattern geometries to test the feasibility of the SMAP technique for creating biologically relevant surface patterns: (a) half-half coated surfaces to judge attachment and motility of the cells on the adhesive (TiO_2 /DDP/proteins) and the nonadhesive (SiO_2 /PLL-*g*-PEG) areas; (b) adhesive patterns of $60 \times 60 \mu\text{m}^2$ size to test the feasibility of organizing

cells on surfaces for applications in areas such as cell-based sensor chips; and (c) adhesive patterns of $5 \times 5 \mu\text{m}^2$ size to investigate the quality of subcellular-sized adhesive patches for localization of focal contacts and organization of cytoskeletal structures. In these cases, adhesion proteins mediating cell attachment spontaneously adsorbed to the DDP domains from the serum contained as a component in the culture medium.

(a) Surface-modified TiO_2 and SiO_2 half-coated samples were seeded with HFFs and incubated in a serum-containing medium. Cell attachment and spreading were monitored after various time intervals by means of phase-contrast microscopy. Cells attached and spread solely on the TiO_2 /DDP surface. They were found to maintain a rounded shape above the SiO_2 /PLL-*g*-PEG surface and were washed away upon medium removal. Furthermore, cells remained on the TiO_2 /DDP side and were not observed to migrate onto the SiO_2 /PLL-*g*-PEG-coated side within the experimental time scale (2 weeks). Tissue-culture polystyrene well plates, as well as untreated, oxide-coated glass cover slides, were used as controls. On both surfaces, cells were found to attach and spread.

(b) Transparent glass as well as Si wafer substrates with adhesive squares of $60 \times 60 \mu\text{m}^2$, separated by $60 \mu\text{m}$, were used to test the suitability of the SMAP technique for immobilization of cells on regular patterns. Cells attached exclusively to the adhesive squares (of size in the order of a single cell) and remained geometrically confined and viable over the entire course of the experiments (2 weeks) (Figure 5,top).

(c) Si wafer substrates with a surface pattern of $5 \times 5 \mu\text{m}^2$ TiO_2 squares in a SiO_2 matrix, separated by $5 \mu\text{m}$, were used in cell experiments to show the suitability of SMAP for creating adhesive patterns with subcellular feature sizes in a nonadhesive background. For visualization of the cell architecture on nontransparent Si wafer

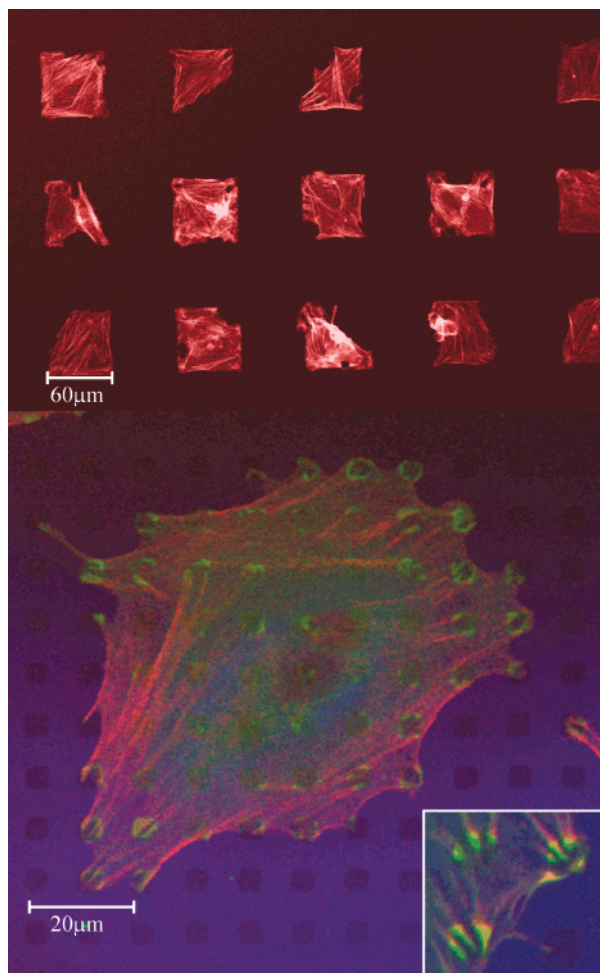


Figure 5. Top: $60 \times 60 \mu\text{m}^2$ of TiO_2 in SiO_2 substrate, SMAP treated. A representative array of fibroblast (HFF) cells attaching to the $60 \times 60 \mu\text{m}^2$ of TiO_2/DDP spots and spreading to the border of $\text{SiO}_2/\text{PLL-g-PEG}$ is shown. Cells were visualized by immunostaining for f-actin. Bottom: HFFs spread on $5 \times 5 \mu\text{m}^2$ TiO_2/DDP cell-adhesive squares in a nonadhesive $\text{SiO}_2/\text{PLL-g-PEG}$ background. Stress fibers were visualized by phalloidin staining for f-actin (red); vinculin was visualized by use of a monoclonal anti-vinculin primary antibody–fluorescently labeled secondary antibody combination (green). Substrate material contrast is visible in reflection mode (blue). The inset shows a magnification of focal contacts formed on the $5 \times 5 \mu\text{m}^2$ adhesive spots.

substrates, stress fibers were stained with rhodamine–phalloidin for f-actin. Vinculin, a protein present on the cytoplasmic side of focal adhesion complexes, was stained to visualize regions of focal contacts to the substrate. It has been previously shown that cells can spread on such surfaces, even when cell–surface contacts are established exclusively on adhesive islands, significantly smaller than that of the projected spread cell.²

HFFs were indeed able to attach and spread on these subcellular patterns but exhibited shapes different from those of cells incubated on nonpatterned substrates. Stress fibers were found to originate mainly above the $5 \times 5 \mu\text{m}^2$ adhesive patterns and often traversed several adhesive patches, while no interaction with the protein-resistant PLL-g-PEG background was evident. Immunostaining for vinculin showed that stress fibers were connected to the focal adhesion sites and that these focal adhesion sites were located exclusively on the $5 \times 5 \mu\text{m}^2$ adhesive features (Figure 5, bottom).

The results of these experiments clearly show that HFF cells consistently recognize the chemical contrast of the

SMAP surfaces. We have strong evidence that this specificity is a direct consequence of the surface chemistry and is not influenced by the small surface topographical features. Due to the lithographic preparation, our substrates contained steps of 30–40 nm between the SiO_2 and TiO_2 areas. The effect of topography was tested in control experiments on $\text{SiO}_2/\text{TiO}_2$ patterned substrates, lacking the organic overlayers. Cells were found to spread freely on the different substrates with no sign of preferential attachment or orientation related to the nanosized step features (data not shown). This finding is consistent with those of earlier studies³⁵ where a topographic variation of 20 nm did not affect cell attachment.

4. Discussion and Conclusions

This report describes a new patterning technique for the preparation of biologically relevant chemical patterns with potential applications in biosensor and implant technologies, as well as in basic investigations of cell behavior. The method is based on selective self-assembly of DDP on TiO_2 , but not SiO_2 , from aqueous solution, in combination with the protein-resistant properties of PLL-g-PEG copolymer adsorbed onto negatively charged metal oxide surfaces. Due to the selective nature of the adsorption of the two adlayers, this technique is termed selective molecular assembly patterning. It relies on well-established sputter deposition, photolithography, and silicon etching techniques to create patterns composed of TiO_2 and SiO_2 areas with required dimensions, the attainable size of which is determined by the resolution of the specific patterning technique involved. The material contrast is then converted, in a series of simple dip-and-rinse processes involving aqueous solutions, into contrast with respect to protein and cell adhesion. This procedure was monitored with XPS and ToF-SIMS specifically used to analyze surface chemical composition, both of which showed unambiguously that DDP adsorbs selectively to the TiO_2 areas and PLL-g-PEG adsorbs to both the bare SiO_2 areas and the DDP-covered TiO_2 areas but proteins adsorb only to the DDP-covered TiO_2 areas, replacing the weakly bound PLL-g-PEG . The resulting contrast with respect to protein adsorption (defined in the results section) was estimated by fluorescence microscopy to be ~ 100 -fold. Human foreskin fibroblasts, cultured in serum-containing media, were consistently found to adhere to the protein-adsorbing structures, where they developed focal contacts and survived for up to 14 days (the experimental time scale). No interaction between the cells and the protein-resistant (PLL-g-PEG) matrix was found within the time frame of the cell-culture experiments. The type of chemical contrast discussed in this report relies on the selective interaction of alkane phosphates with TiO_2 (or a number of other transition metal oxides) but not with SiO_2 surfaces. This is only one possible means of contrast formation within the frame of the SMAP technology. Strategies based on pH-dependent electrostatic contrast are currently being explored. Another area of interest is the extension of pattern size from the micrometer to the submicrometer or nanometer range, requiring substrates with finer oxide prepatterns that can be produced with the help of more sophisticated photolithographic techniques such as deep UV, X-ray, interference or colloidal particle lithography, electron beam lithography, or focused ion beam structuring.

SMAP presents a number of advantages, of particular relevance to an industrial environment, over the estab-

(35) Scotchford, C.; Winkelmann, M.; Gold, J.; Textor, M. *Biomaterials*, in preparation.

lished patterning techniques. First, the biologically relevant molecular adlayers form via a sequence of simple dip-and-rinse processes. No complex surface functionalization and immobilization schemes are required. Second, the production of required patterned oxide substrates is based on standard lithographic techniques. They are used to produce the required metal oxide patterns and do not cause any of the technological problems often encountered in alternative approaches based on photolithographic patterning of organic overlayers, where residual solvents can lead to inhomogeneities and degradation of the organic overlayers. These advantages of the SMAP technique, in turn, translate into cost-effectiveness, reproducibility, and compatibility with large-scale production of contamination-free chips bearing the desired biologically relevant patterns.

The SMAP technology has a number of potential applications, particularly in the area of microarray biosensor chips for DNA/RNA (genomics) or protein (proteomics) sensing, by providing patterns with defined physicochemical properties for improved spotting of recognition molecules and for cell-based sensor chips that require the provision of stable cell-adhesive areas on a highly protein- and cell-resistant background.

Acknowledgment. We thank Michael Horisberger for providing the sputter-coated oxide substrates and Paul Hug for help with the ToF-SIMS measurements and evaluation. Dr. Andreas Goessl, Dr. Janos Vörös, and Dr. Louis Tiefenauer are thanked for stimulating discussions.

LA011715Y